$B_s \to \gamma\gamma$ decay in the two-Higgs-doublet model

T. M. Aliev* and G. Turan
Physics Department, Middle East Technical University, 06531 Ankara, Turkey
(Received 10 February 1993)

The rare $B_s \to \gamma\gamma$ decay has been investigated in the framework of the two-Higgs-doublet model. It is shown that the branching ratio has a great enhancement in comparison to the standard model (SM) prediction. We have found that the ratio of the square of the CP=1 to $CP = -1$ amplitudes, $|A^+|^2/|A^-|^2$, which is always less than one in the SM, becomes greater than one for some values of m_H/m_t. We have also calculated the direct CP-violating parameter $\epsilon'_{\gamma\gamma(-)}$. It is found that for $K \to \gamma\gamma$ decay its value is greater than the one which follows from the SM, while for $B_s \to \gamma\gamma$ decay both models have the same predictions. Finally, we compare our results on $B_s \to \gamma\gamma$ decay with the results of $B_s \to \mu^+\mu^-$ and $B_s \to \mu^+\mu^-$ decays which are of the same order of the coupling constant.

PACS number(s): 13.40.Hq, 11.30.Er, 12.15.Cc, 14.40.Jz

I. INTRODUCTION

The theoretical and experimental investigations of the rare decays are one of the main research fields of the particle physics. In the standard model (SM), rare decays take place at the one-loop level. Thus they may provide a precise test for the higher-order structure of the SM. Since rare decays are also sensitive to the presence of the new physics, they are one of the promising objects for establishing the physics beyond the SM.

This paper is devoted to the study of $B_s \to \gamma\gamma$ decay in two-Higgs-doublet model. The reason of choosing the $B_s \to \gamma\gamma$ decay may be summarized as follows. First, in this decay short-distance effects likely dominate so that theoretical calculations are more reliable. Second, since as is well known, a two-photon system can be in a CP-even or in a CP-odd state, the $B_s \to \gamma\gamma$ decay allows one for the study of CP violation.

There are many theoretical reasons why we need two-Higgs-doublet models. First of all, these models are dictated by the supersymmetry which requires at least two scalar doublets [1] and also by the solution of the strong CP problem (Peccei-Quinn mechanism) [2]. Another reason is to provide a mechanism for the mass differences between up- and down-type quarks through the Yuakawa coupling, where one of the doublets generates masses of the up quarks and the other one generates masses of the down quarks. (For more about two-Higgs-doublet models, see, for example, [3].)

We note that this decay has been previously investigated in the framework of the SM [4,5]. In this work, we will consider the minimal extension of the SM, namely, by adding one complex Higgs doublet to avoid the large number of new undetermined parameters of the theory.

The plan of the paper is as follows. In Sec. II, we present the one-loop calculations for the $B_s \to \gamma\gamma$ decay in the quark level. Here we have used the Feynman–'t Hooft gauge and the on-shell renormalization scheme. The numerical results and discussion are given in Sec. III.

II. DECAY $B \to S\gamma\gamma$

At quark level the decay $B_s \to \gamma\gamma$ takes place via a $b \to s\gamma\gamma$ transition, which is described by the Feynman diagrams shown in Fig. 1. The transition amplitude for $b \to s\gamma\gamma$ decay can be written as

$$M = \epsilon_\mu(k_1)\,\epsilon_\nu(k_2)\,\bar{u}(p')\,T_{\mu\nu}\,u(p)\ , \tag{1}$$

where $\epsilon_\mu(k_1)$ and $\epsilon_\nu(k_2)$ are the four vector polarizations of the photons. At the lowest order of perturbation theory, $T_{\mu\nu}$ receives contributions from flavor-changing reducible and irreducible diagrams, which are presented in Fig. 1, and it can be written as

$$T_{\mu\nu} = \sum_{\ell=u,c,t} V_{\ell b}\,V^*_{\ell s}\,T_{\ell\mu\nu}\ , \tag{2}$$

where $V_{\ell q}$ is the corresponding Kobayashi-Maskawa (KM) matrix element. Using the unitarity condition for

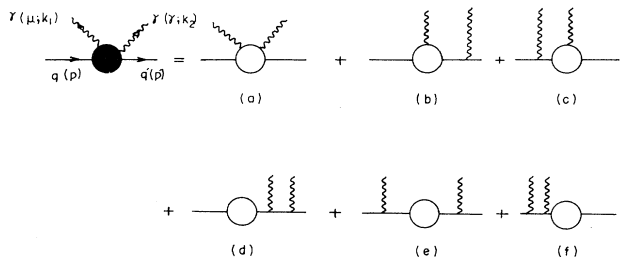

FIG. 1. Feynman diagrams responsible for the $q \to q'\gamma\gamma$ decay. Here solid lines denote fermions, wavy ones photons.

*Permanent address: Institute of Physics, Azerbaijanian Academy of Sciences, Baku, Azerbaijan.

KM matrix we can decompose the contributions to $T_{\mu\nu}$ into the CP-conserving and CP-violating parts:

$$T_{\mu\nu} = V_{ub} V_{us}^* (T_{u\mu\nu} - T_{c\mu\nu}) - V_{tb} V_{ts}^* (T_{c\mu\nu} - T_{t\mu\nu}) \ . \quad (3)$$

The CP-violating quantity $\epsilon'_{\gamma\gamma(-)}$ (for its definition, see, for example, [5]) requires calculation of the reducible and irreducible diagrams. So we should first calculate $T_{\ell\mu\nu}$ to find the transition amplitude of the $q_i \to q_j \gamma\gamma$. Before doing this we would like to make some remarks. Since in the two-Higgs-doublet model which we apply in this work physical charged Higgs fields are present, one should also consider the interaction between charged Higgs fields and quarks. Note that in these models large flavor-changing neutral currents (FCNC's) are present due to the neutral boson exchanges. There are two ways to avoid them, each involving some discrete symmetry. In the first way, all the quarks couple only to one of the Higgs doublets (model I), while in the second way down quark couples to one of the Higgs doublets and up quarks couples to the other one (model II) [6, 7]. In terms of the mass eigenstates the interaction Lagrangian between physical charged Higgs bosons and the fermions has the form

$$L = \frac{g}{\sqrt{2}\, M_W} [m_{u_i}\, \xi\, \bar{u}_i\, L\, d_j - m_{d_i}\, \xi'\, \bar{u}_i\, R\, d_j]\, V_{ij}\, H^+ + \text{H.c.} \ , \quad (4)$$

where $L = (1-\gamma_5)/2$, $R = (1+\gamma_5)/2$, g is the weak coupling, ξ and ξ' are the ratios of the two vacuum expectation values (VEV's) v_1 and v_2, and m_{u_i} (m_{d_i}) are the masses of the up (down) quarks. In the above-mentioned models,

$$\xi' = -\frac{1}{\xi} \quad \text{(model I)} \ ,$$

$$\xi' = \xi \quad \text{(model II)} \ .$$

Note that the interaction Lagrangian between unphysical charged Higgs bosons and fermions is the same as the one in the standard model case. From Fig. 2 we see that the new interaction (4) will receive contributions from the diagrams of Figs. 2(a)–2(g). Note that model I can be realized in supersymmetric theories (see, for example, [8]) or in a Peccei-Quinn-type symmetry.

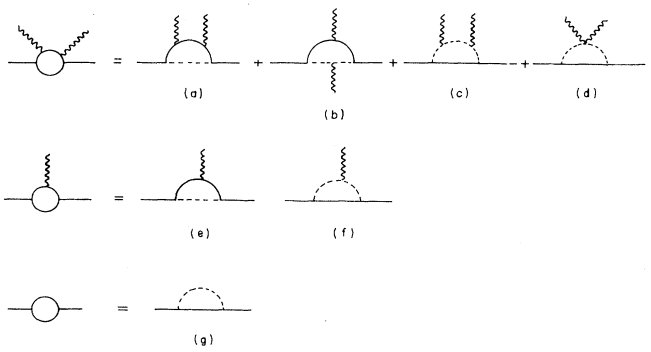

FIG. 2. Flavor-changing irreducible and reducible diagrams. Here dashed lines denote the W boson and Higgs boson (physical and unphysical).

Now we say a few words about the CP-violating vertex. It is well known that two-Higgs-doublet models in general have additional flavor-diagonal CP-violating vertices due to the interaction between neutral Higgs bosons and quarks (see, for example, [9]). But in the flavor-changing decays, CP violation via neutral Higgs-boson exchanges appears in the higher orders and for this reason it is suppressed in comparison to the CP violation via the KM phase. Therefore, we shall not take into account this possibility.

Let us now calculate the contributions to $T_{\mu\nu}$ coming from the irreducible and reducible diagrams.

A. Irreducible diagrams

Here we refer to the diagrams of Fig. 2. Note that in the internal quark lines we only consider the top quark because in the charged Higgs exchange diagrams contributions from the light quarks are suppressed by a factor of m_q/M_W. Since the mass of the top quark is much larger than all the external masses and momenta, terms such as m_q^2/M_W^2 and m_q^2/m_t^2 can be neglected. Calculations for the irreducible diagrams leads to the result

$$\begin{aligned} T_{t\,\mu\nu} = {} & \frac{g^2 e^2 e_H^2}{16\pi^2} \frac{m_t^2}{2M_W^2} \{ \xi^2\, I(2;1) [\gamma_\mu L (2p - k_1 - k_2)_\nu \\ & + \gamma_\nu L (2p - k_1 - k_2)_\mu + g_{\mu\nu} (2\hat{p} - \hat{k}_1 - \hat{k}_2) L] - 2\xi\xi' I(1;1)(m_i R + m_j L)\} \\ & + \frac{g^2 e^2 e_t^2}{16\pi^2} \frac{m_t^2}{2M_W^2} \{\xi^2 I(2;1)[\gamma_\mu(\not{p} - \not{k}_2)\gamma_\nu L + \gamma_\nu (\not{p} - \not{k}_1)\gamma_\mu L \\ & + 2g_{\mu\nu} (m_i R + m_j L)] + \xi^2 I(1;2)[\gamma_\mu(\hat{k}_1 - \hat{k}_2)\gamma_\nu - \gamma_\nu(\hat{k}_1 - \hat{k}_2)\gamma_\mu]L \\ & - 2\xi\xi' g_{\mu\nu} I(1;1) (m_i R + m_j L) \} \\ & + \frac{g^2 e_u^2 e_H^2}{16\pi^2} \frac{m_t^2}{2M_W^2} \xi^2 \{ I(2;1)[\gamma_\mu(2\not{p} - \not{k}_1 - \not{k}_2)\gamma_\nu + \gamma_\nu (2\not{p} - \not{k}_1 - \not{k}_2)\gamma_\nu \\ & + 4g_{\mu\nu}(2\not{p} - \hat{k}_1 - \hat{k}_2)] + \tfrac{1}{2} I(1;1)[\gamma_\mu(\hat{k}_1 - \hat{k}_2)\gamma_\nu - \gamma_\nu(\not{k}_1 - \not{k}_2)\gamma_\mu] \} L \ , \end{aligned} \quad (5)$$

where

$$I(\alpha;\beta)=\int_0^1 \frac{x^\alpha(1-x)^\beta}{m_t^2(1-x)+m_H^2\,x}\,dx\ . \tag{6}$$

B. Reducible diagrams

Reducible diagrams are of two types: the self-energy and the vertex diagrams as shown in Fig. 2. One can write the contributions of these diagrams as

$$\begin{aligned}T_{t\,\mu\nu}=&-e\,e_d\,[\gamma_\nu\,S(p'+k_2,m_j)\,\Gamma_\mu\,(p,p-k_1,k_1)+\Gamma^\nu\,(p'+k_2,p',k_2)\,S(p-k_1,m_i)\,\gamma_\mu]\\&+(ee_d)^2\,[\gamma_\mu\,S(p'+k_2,m_j)\,\gamma_\mu\,S(p,m_j)\,\Sigma(p)+\Sigma(p')\,S(p',m_i)\,\gamma_\nu\,S(p-k_1,m_i)\gamma_\mu\\&\qquad+\gamma_\nu S(p'+k_2,m_j)\,\Sigma(p-k_1)\,S(p-k_1,m_i)\,\gamma_\mu]\\&+\{k_1\leftrightarrow k_2,\mu\leftrightarrow\nu\}\ ,\end{aligned} \tag{7}$$

where $S(p,m)=(p-m)^{-1}$ and Σ and Γ are the self-energy and vertex operators. In the on-shell renormalization scheme, the renormalized self-energy and vertex operators in Eq. (7) have the forms

$$\Sigma(p)=(\not p'-m_j)\,\hat\Sigma(\not p-m_i)\ , \tag{8}$$

$$\Gamma_\mu(p,p',k)=[F_1(k^2\gamma_\mu-k_\mu\ \not k)\,L-iF_2\,\sigma_{\mu\nu}\,k_\nu\,(m_iR+m_jL)+(\not p'-m_j)\,O_{1\mu}(p,p',k)+O_{2\mu}(p,p',k)\,(\not p-m_i)]\ . \tag{9}$$

Here F_1 and F_2 correspond to the charge-radius and dipole momentum terms, respectively. After some calculations we get, for $\hat\Sigma$ and Γ_μ,

$$\hat\Sigma(p)=\frac{g^2}{16\pi^2}\,\frac{m_t^2}{2M_W^2}\{\,\xi^2(\not pR+m_jL+m_iR)I(2;1)-\xi\xi'(m_jR+m_iL)I(1;1)\} \tag{10}$$

and

$$\begin{aligned}\Gamma_\mu=&-\frac{g^2e\,e_u}{16\pi^2}\,\frac{m_t^2}{2M_W^2}\,\xi^2\Big\{-i\,\frac{I(2;1)}{2}\sigma_{\mu\nu}\,k_\nu(m_i\,R+m_j\,L)-(\not k k_\mu-k^2\gamma_\mu)\,L\,\frac{1}{6}\,[\,(2I(0;2)+I(1;2)]\\&-(\hat p-\hat k-m_j)\{[(\hat p-\hat k)R+m_jR+m_iL]\gamma_\mu I(2;1)+(k_\mu-\gamma_\mu\ \not k)\,L\,\tfrac12 I(1;2)\}\\&-(\not p-m_i)\,[\gamma_\mu(\not pR+m_jR+m_iL)I(2;1)-(k_\mu-\not k\gamma_\mu)R\,\tfrac12\,I(1;2)]\\&-(\not p-\not k-m_j)\gamma_\mu R\,(\not p-m_i)I(2;1)\Big\}\\&-\frac{g^2e\,e_u}{16\pi^2}\,\frac{m_t^2}{2M_W^2}\,\xi\xi'\{\,-i\,I(0;2)\sigma_{\mu\nu}\,k_\nu(m_i\,R+m_j\,L)\\&\qquad+I(1;1)[\,(\not p-\not k-m_j)\gamma_\mu(m_iR+m_jL)+\gamma_\mu(m_iL+m_jR)(\not p-m_i)]\}\\&-\frac{g^2e\,e_H}{16\pi^2}\,\frac{m_t^2}{2M_W^2}\{\,(\not p-\not k-m_j)(\,\xi'^2\{\,-I(2;1)[(\not p-\not k)R+m_jR+m_iL]\gamma_\mu\\&\qquad+k_\mu L\,[\tfrac12 I(2;0)-\tfrac23 I(3;0)]-\tfrac12 I(2;1)\ \not k\gamma_\mu L\}+\xi\xi'\gamma_\mu(m_jL+m_iR)I(1;1))\\&+(\not p-m_i)(\xi'^2\{\,-I(2;1)\gamma_\mu(\not pR+m_iL+m_jR)-\tfrac12\ \not k\gamma_\mu R\,I(2;1)\\&\qquad+k_\mu R[I(2;1)-\tfrac12 I(2;0)+\tfrac23 I(3;0)]\}+\xi\xi'(m_jL+m_iR)\gamma_\mu I(1;1))\\&+\xi'^2[\tfrac16 I(3;0)(k_\mu\ \not kL-k^2\gamma_\mu L)-I(2;1)(\not p-\not k-m_j)\gamma_\mu R(\not p-m_i)\\&\quad-\tfrac12 I(2;1)i\sigma_{\mu\alpha}k_\alpha(m_iR+m_jL)+\xi\xi'I(1;1)i\sigma_{\mu\alpha}k_\alpha(m_iR+m_jL)]\}\ .\end{aligned} \tag{11}$$

Taking into account the explicit forms of Eqs. (8)–(11) we find that the sum of Eqs. (5) and (7) for on-shell quarks and photons can be written in terms of the dipole moment form factor F_2:

$$T_{t\,\mu\nu}=-\frac{g^2e^2}{16\pi^2}\,\frac{m_t^2}{2M_W^2}\,\frac{i}{2}\,\Big\{\,e_u\,e_d\,[-\xi^2\,I(1;2)+2\xi\,\xi'\,I(0;2)]\,+\,e_H\,e_d\,\left[\xi^2\,I(2;1)-2\xi\,\xi'\,I(1;1)\right]\,\Big\}\,W\ ; \tag{12}$$

where the nonlocal operator W is defined by

$$W = (m_i R + m_j L)\Bigg\{ -\left[\left(\frac{p'_\mu}{p' k_1} - \frac{p_\mu}{p k_1}\right)\sigma_{\mu\alpha} k_{2\alpha} + \left(\frac{p'_\nu}{p' k_2} - \frac{p_\nu}{p k_2}\right)\sigma_{\mu\beta} k_{1\beta}\right] + \frac{i}{2}\left[\left(\frac{1}{p' k_2} - \frac{1}{p k_1}\right)\sigma_{\nu\beta} k_{2\beta}\sigma_{\mu\alpha} k_{1\alpha} + \left(\frac{1}{p' k_1} - \frac{1}{p k_2}\right)\sigma_{\mu\alpha} k_{1\alpha}\sigma_{\nu\beta} k_{2\beta}\right]\Bigg\} . \tag{13}$$

It is interesting to note that contributions from Σ and a part of Γ cancel completely with contributions from the irreducible diagrams. In other words, the decay amplitude is totally defined by the vertex operators. This happens in the standard model also [4, 5].

Equation (12) is the final result of the quark-level calculations. We note that our calculations do not include QCD corrections. This requires a complete analysis because of the following reasons. First, the operators appearing in the $b \to s\gamma\gamma$ decay, unlike the $b \to s\gamma$ case, are highly nonlocal. Second, the complete set of the operators are rather large. However, we expect that these corrections will not change our results significantly.

We now use Eq. (12) to find the matrix element of the $M \to \gamma\gamma$ decay ($M = B, K \ldots$). The appearance of the nonlocal operators in (12) makes the decay process very sensitive to the model used for the meson wave function. As it seems, for a heavy-meson decay short-distance effects are dominant and we use the static quark approximation to estimate them [4, 5, 10]. (This means that we use the constituent masses of the quarks.) In this approximation, we have, for the nonlocal operator W defined in Eq. (13),

$$W = \frac{2i}{m_M}\left(\frac{1}{m_i} + \frac{1}{m_j}\right)(-g_{\mu\nu} k_1 k_2 + k'_{1\nu} k_{2\mu} - i\epsilon_{\mu\nu\alpha\beta} k_{1\alpha} k_{2\beta}\gamma_5) . \tag{14}$$

Using the standard definition

$$\langle 0 \mid \bar{q}_j \gamma_\mu \gamma_5 q_i \mid M \rangle = -i f_M p_M , \tag{15}$$

we get the following final result for the decay amplitude:

$$A = -\frac{\alpha G_F}{\sqrt{2}\pi} f_M \left[A^+ F_{\mu\nu} F_{\mu\nu} + i A^- F_{\mu\nu}\tilde{F}_{\mu\nu}\right] . \tag{16}$$

Here $F_{\mu\nu}$ is the electromagnetic-field tensor, $\tilde{F}_{\mu\nu} = \frac{1}{2}\epsilon_{\mu\nu\alpha\beta} F_{\alpha\beta}$, f_M is the M-meson decay constant, and

$$A^+ = \sum_{n=u,c,t} V_{ni} V^*_{nj} \frac{M_M}{6}\left(\frac{1}{m_i} + \frac{1}{m_j}\right)\left(\frac{m_i - m_j}{m_i + m_j}\right)\left[F_2^{\rm SM}(\alpha_n) + F_2^H(\beta_n)\right] ;$$

$$A^- = \sum_{n=u,c,t} V_{ni} V^*_{nj}\left[\frac{4}{9}\delta_3(z_n) - \frac{M_M}{6}\left(\frac{1}{m_i} + \frac{1}{m_j}\right)\left[F_2^{\rm SM}(\alpha_n) + F_2^H(\beta_n)\right]\right] , \tag{17}$$

which correspond to $CP = 1$ and $CP = -1$ amplitudes, respectively. Here $\alpha_n = m_n^2/M_W^2$, $\beta_n = m_n^2/m_H^2$, and $z_n = m_n^2/M_M^2$. The quantities δ_3 and $F_2^{\rm SM}$ are given in Ref. [4] as

$$\delta_3(z_n) = 1 + \frac{2}{z_n} G(z_n) , \tag{18}$$

where

$$G(z_n) = \begin{cases} -2\arctan^2\sqrt{\frac{z_n}{4-z_n}} & \text{if } z_n < 4 , \\ -\frac{\pi^2}{2} + 2\ln^2\left(\frac{\sqrt{z_n}+\sqrt{z_n-4}}{z_n}\right) - 2i\pi\ln\left(\frac{\sqrt{z_n}+\sqrt{z_n-4}}{z_n}\right) & \text{if } z_n > 4 , \end{cases}$$

and

$$F_2^{\rm SM}(x) = \frac{1}{36(1-x)^4}\left[-46 + 205x - 312x^2 + 175x^3 - 22x^4 + 18x^2(2-3x)\ln x\right] . \tag{19}$$

We have found that

$$F_2^H(x) = \frac{x}{36(1-x)^4}\left\{\xi^2\left[7 - 12x - 3x^2 + 8x^3 + 6x(2-3x)\ln x\right] + 6\xi\,\xi'(1-x)\left[3 - 8x + 5x^2 + 2(2-3x)\ln x\right]\right\} , \tag{20}$$

which follows from Eq. (12).

Using Eq. (16), we obtain, for the partial decay width,

$$\Gamma(M \to \gamma\gamma) = \frac{m_M^3}{16\pi} \left(\frac{\alpha G_F}{\sqrt{2}\pi} f_M\right)^2 (|A^+|^2 + |A^-|^2) . \tag{21}$$

From Eq. (18) we have, for $B_j \to \gamma\gamma$ decay,

$$A^+ = -V_{tb} V_{tj}^* \frac{M_B}{6m_j} \left[F_2^{\rm SM}(\alpha_c) - F_2^{\rm SM}(\alpha_t) - F_2^H(\beta_t)\right] ,$$

$$A^- = -V_{tb} V_{tj}^* \left[\frac{4}{9}\delta_3(z_c) - \frac{M_B}{6m_j}[F_2^{\rm SM}(\alpha_c) - F_2^{\rm SM}(\alpha_t) - F_2^H(\beta_t)]\right] + V_{ub} V_{uj}^* \frac{4}{9}[\delta_3(z_u) - \delta_3(z_c)] , \tag{22}$$

where m_j are the constituent masses of the corresponding quarks. Deriving the above expression we have used the unitarity of Cabibbo-KM (CKM) matrix, neglecting the $\delta_3(\alpha_t)$ contribution, which is numerically small in comparison with $\delta_3(\alpha_c)$. In addition, we take the $F_2^{\rm SM}(\alpha_u) - F_2^{\rm SM}(\alpha_c) = 0$ that follows from the the Glashow-Iliopoulos-Maiani (GIM) mechanism. Since $V_{ub} V_{us}^* \ll V_{tb} V_{ts}^*$, the second part of the A^- can be neglected in the $B_s \to \gamma\gamma$ decay. But in the $B_d \to \gamma\gamma$ case, the above-mentioned matrix elements are of the same order of magnitude so that both of the terms in A^- should be taken into account. From Eq. (21) it follows that

$$\frac{B(B_d \to \gamma\gamma)}{B(B_s \to \gamma\gamma)} \approx \frac{|V_{td}|^2}{|V_{ts}|^2} \frac{(f_{B_d})^2}{(f_{B_s})^2} \simeq \frac{|V_{td}|^2}{|V_{ts}|^2}(1+\delta) ,$$

where δ is an SU(3)-breaking parameter. Using the present bound $|V_{td}|^2/|V_{ts}|^2 \leq 0.16$ one expects that $B_d \to \gamma\gamma$ decay is suppressed in comparison to $B_s \to \gamma\gamma$ decay at least by a factor of 0.16.

In addition to measuring the width of the $B \to \gamma\gamma$ decay, another way of exploring the influence of m_t and m_H on it would be to measure the photon spin polarization. In the rest frame of the meson the $CP = -1$ amplitude A^- is proportional to the perpendicular-spin polarization $\boldsymbol{\varepsilon}_1 \times \boldsymbol{\varepsilon}_2$, while the $CP = 1$ amplitude A^+ is proportional to the parallel-spin polarization $\boldsymbol{\varepsilon}_1 \cdot \boldsymbol{\varepsilon}_2$ of the photons. It is well known that at $m_t \geq m_W$ both amplitudes are important and potentially this would lead to a CP violation.

We conclude this section by writing out the values of parameters we have used in the numerical analysis: $|V_{tb}V_{ts}^*| \simeq 5 \times 10^{-2}$, $f_{B_s} = 140$ MeV obtained from the QCD sum rules[1] [11]. We assume that the decay rate

[1]If we choose a larger value for f_{B_s} (for example, $f_{B_s} = 190$ MeV or $f_{B_s} \approx 300$ MeV, which follow from the effective heavy-quark theory [12] and lattice QCD calculations [13], respectively), then B increases by a factor of $(f_{B_s}/140\ \text{MeV})^2$.

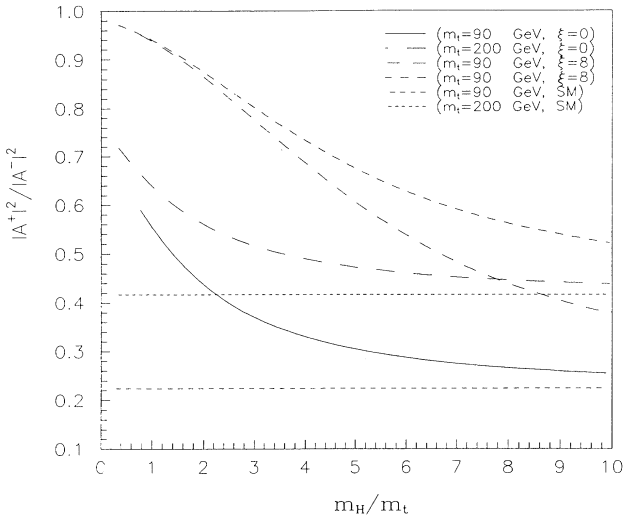

FIG. 3. Dependence of the square of the ratio of the $CP = 1$ to $CP = -1$ amplitudes, $|A^+|^2/|A^-|^2$, on m_H/m_t in model I. Here SM denotes the standard model prediction.

width is the same as the total decay width of the B meson, and we use the experimental value of $\Gamma_B \simeq 3 \times 10^{-4}$ eV [14].

The free parameters of the two-Higgs-doublet model which we have used are ξ, ξ', and m_{H^+}. However, there are some constraints on them by the existing experimental data. Recent analysis of the data from B and K physics and CP violation [15], as well as the unitarity and perturbative considerations [16], lead to the restrictions

$$0.1 \leq \frac{1}{\xi} \leq \min\left(150\ \text{GeV}, \frac{0.9}{m_{H^+}}\ \text{GeV}\right) ,$$
$$m_H \geq \tfrac{1}{2} m_Z . \tag{23}$$

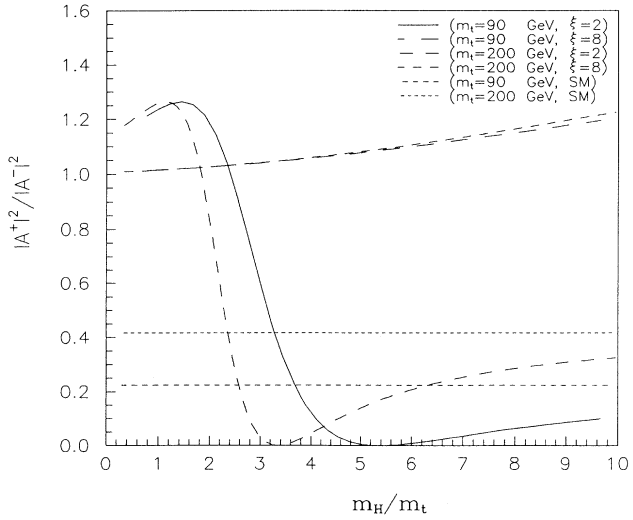

FIG. 4. Same as Fig. 3, but in model II.

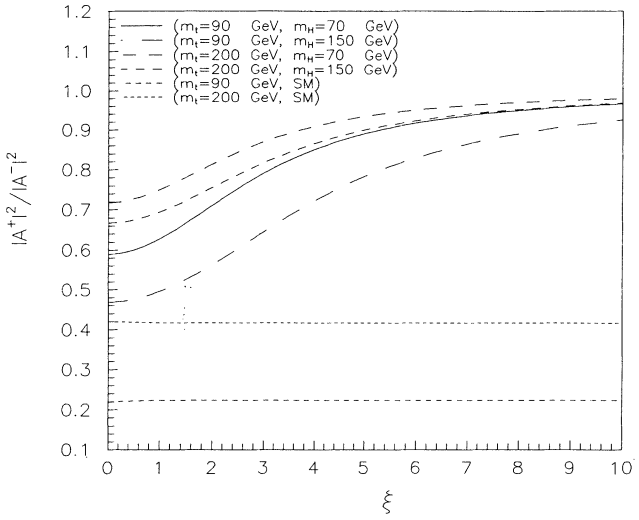

FIG. 5. Dependence of the $|A^+|^2/|A^-|^2$ on ξ in model I.

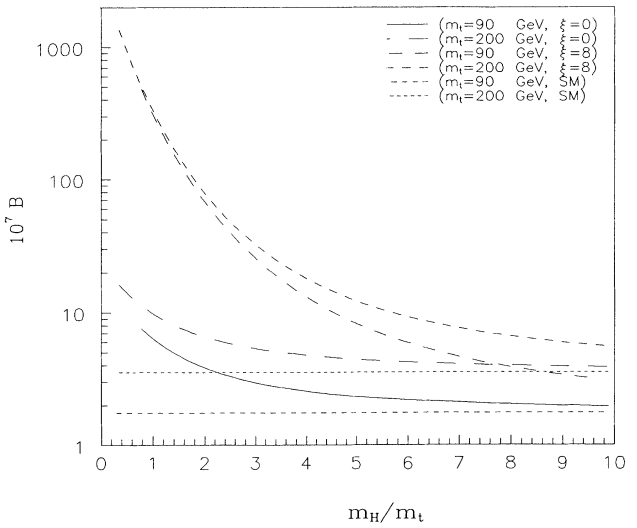

FIG. 7. Dependence of the $B(B_s \to \gamma\gamma)$ on m_H/m_t in model I.

III. RESULTS AND DISCUSSION

We have chosen to present a number of representative results in a series of graphs. (Figs. 3–12). In Figs. 3 and 4, we plot the dependence of the square of the ratio of the $CP = 1$ to the $CP = -1$ amplitudes, $|A^+|^2/|A^-|^2$, on the m_H/m_t at some fixed values of the ξ and m_t. The interesting result which follows from this figure is that there are some values of m_H/m_t where the ratio $|A^+|^2/|A^-|^2 > 1$. This result contradicts the SM predictions where the above-mentioned ratio is always less than 1, and it may open a "window" for investigating the CP violation in $B_s \to \gamma\gamma$ decay. From Figs. 3 and 4 we also see that for $m_H/m_t \gg 1$, the ratio $|A^+|^2/|A^-|^2$ tends to SM predictions in both models. (Note that in model II, ξ gets only large values, while in model I it is possible large as well as small values of ξ [15].) We have also plotted the ratio $|A^+|^2/|A^-|^2$ as a function of the parameter ξ in Figs. 5 and 6. It is seen from these figures that the two-Higgs-doublet model predictions about this ratio mainly exceed the SM ones. Referring to Fig. 6, we note that the behavior of being greater than 1 can be clearly observed for the ξ dependence of the $|A^+|^2/|A^-|^2$ too in model II.

Figures 7 and 8 show the dependence of the B on m_H/m_t in models I and II, respectively. From these figures it follows that for $m_H \sim m_t$ the B gets large enhancement. It is interesting to note that in model II there are some m_H/m_t and ξ regions where the predictions of the two-Higgs-doublet model are strongly suppressed in comparison to the SM predictions. This is because the F_2^H terms dominate $F_2^{\rm SM}$ ones for large ξ and, in model II, $\xi\xi' = \xi^2$, and the sign of F_2^H is opposite to that of

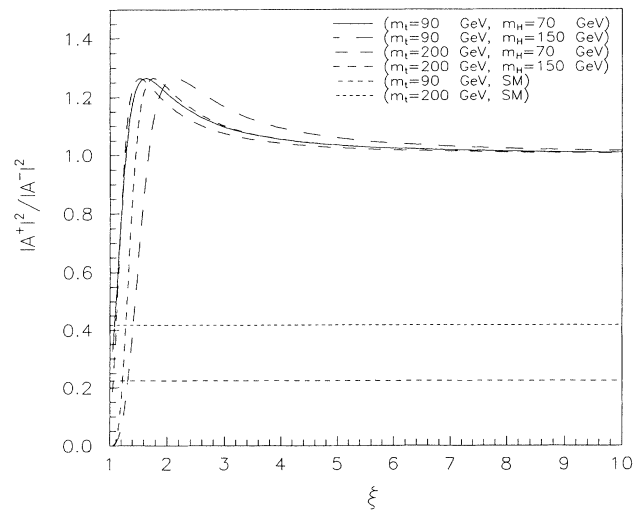

FIG. 6. Same as Fig. 5, but in model II.

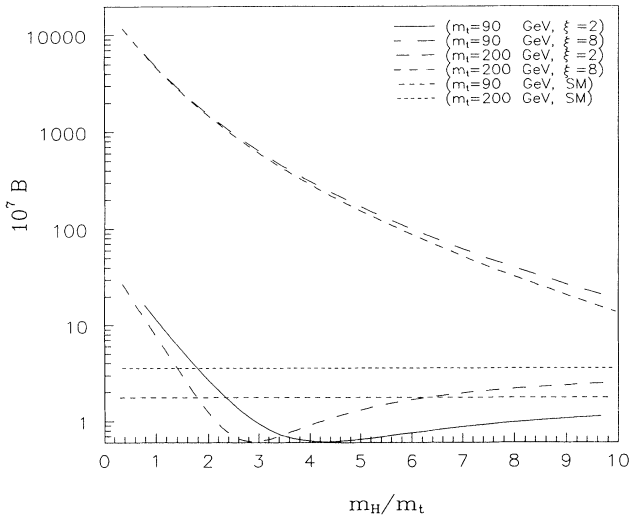

FIG. 8. Same as Fig. 7, but in model II.

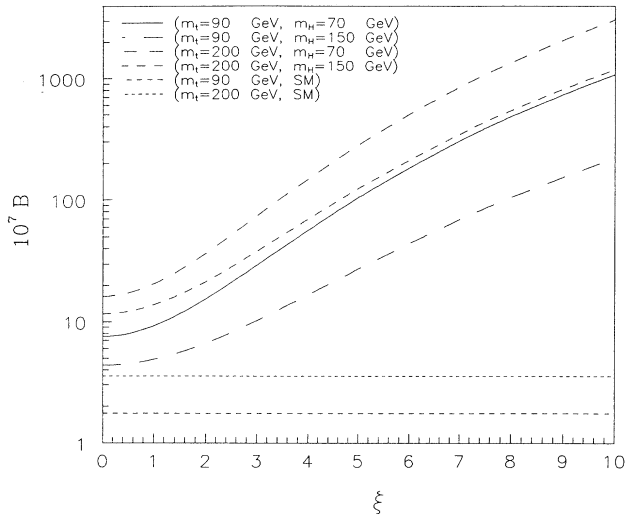

FIG. 9. Dependence of the $B(B_s \to \gamma\gamma)$ on ξ in model I.

$F_2^{\rm SM}$ in Eqs. (19) and (20). In other words, in model II at some values of ξ and m_H/m_t, F_2^H gives destructive interference to $F_2^{\rm SM}$. We see from Fig. 8 that, for $m_t = 200$ GeV and $\xi = 2, 8$, B has the order of $10^{-4} - 10^{-5}$ in the region of $2 \leq m_H/m_t \leq 5$. This value is two to three orders of magnitude greater than the SM predictions so that B for $B \to \gamma\gamma$ is quite detectable in the future B-meson factories. (Remember that at $m_t = 200$ GeV, $B^{\rm SM} \sim 10^{-7} - 10^{-8}$.)

We present the dependence of the B on ξ for different values of the m_t and m_H in Figs. 9 and 10. It follows from Fig. 9 that, in model I, $B \geq 10^{-6}$ usually, while in model II (Fig. 10) it is strongly suppressed in comparison to the SM case at some ξ regions.

Here we would like to make some comments about the direct CP-violating parameter $\epsilon'_{\gamma\gamma(-)}$. First, we want to

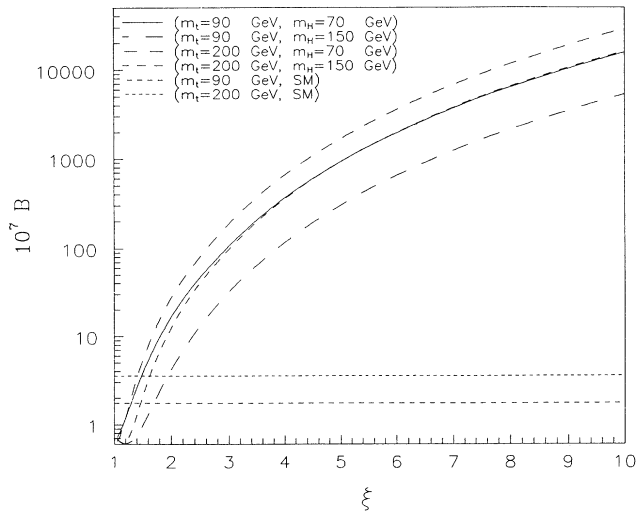

FIG. 10. Same as Fig. 9, but in model II.

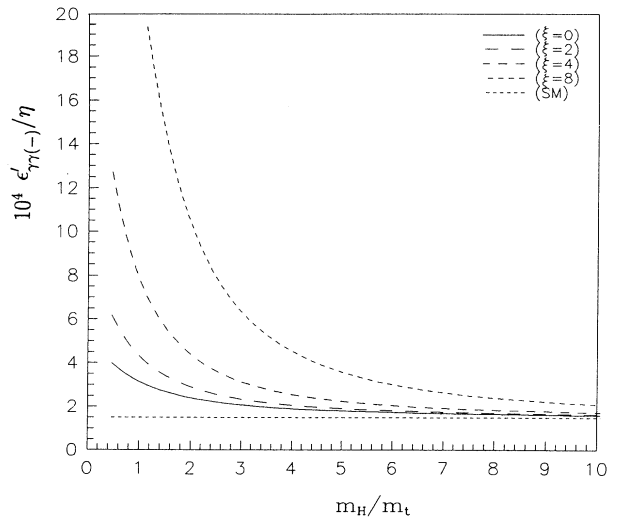

FIG. 11. Graph of the $\epsilon'_{\gamma\gamma(-)}/\eta$ vs m_H/m_t at $m_t = 150$ GeV in model I.

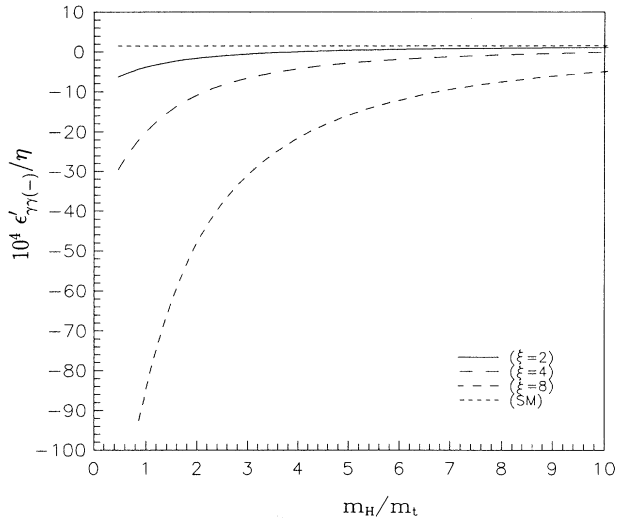

FIG. 12. Same as Fig. 11, but in model II.

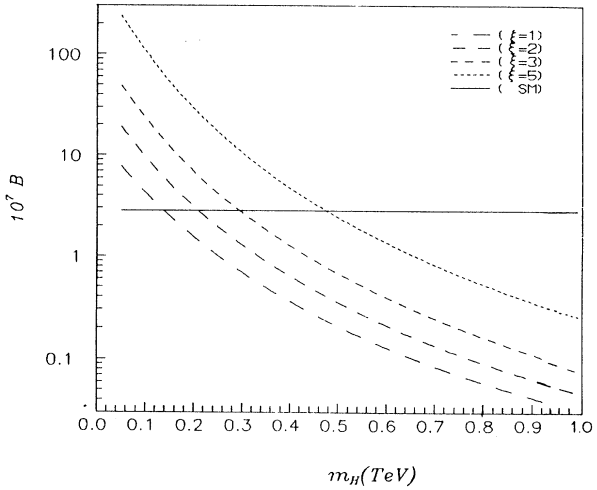

FIG. 13. Dependence of the $B(B_s \to \gamma\gamma)$ on m_H at $m_t = 150$ GeV in model I in the case that the amplitude gets contribution only from the charged Higgs bosons.

discuss this parameter in $K \to \gamma\gamma$ decay. In this case the term $V_{ts}V_{td}^*$ is small in comparison to $V_{us}V_{ud}^*$, and so it is likely that a light u-quark contribution becomes dominant. Therefore long-distance effects are very essential to calculate the decay amplitude. For this reason we shall use the emprical value $A_{\rm phys} = 3.6$ in Eq. (3) instead of the $T_u - T_c$ contribution. Another point to mention is that the appearance of the nonlocal operator W makes it very difficult to give reliable estimates about $\epsilon'_{\gamma\gamma(-)}$. Therefore, we can calculate its order of magnitude in K-meson decay. Taking the constituent quark masses as $m_d = 300$ MeV and $m_s = 500$ MeV we get

$$\epsilon'_{\gamma\gamma(-)} = \frac{\mathrm{Im}(V_{ts}V_{td}^*)\left\{\frac{8}{9}\left[\delta_3(z_c) - \delta_3(z_t)\right] - 0.8[F_2^{\rm SM}(\alpha_c) - F_2^{\rm SM}(\alpha_t) - F_2^H(\beta_t)]\right\}}{\mathrm{Re}(V_{us}V_{ud}^*)\, A_{\rm phys}} \,. \tag{24}$$

Calculations show that the δ_3 terms are small in comparison to the F_2's, so that they can be neglected. In the numerical calculations we have used the following values for the CKM parameters λ, A, ρ, and η (Wolfenstein parametrization [17] has been used)

$$\lambda = |V_{us}| = 0.2205 \pm 0.0018 \,,$$
$$A = 0.90 \pm 0.12 \,,$$
$$0.2 < \eta < 0.5 \,.$$

(These numerical values are taken from Ref. [18].) In Figs. 11 and 12 we present the graph of $\epsilon'_{\gamma\gamma(-)}/\eta$ versus m_H/m_t for some different values of the parameter ξ at $m_t = 150$ GeV. We see from Fig. 11 that, in model I, $\epsilon'_{\gamma\gamma(-)}/\eta$ is 2–15 times greater than the SM prediction for $0 \le \xi \le 8$ and $m_H \simeq m_t$. We observe a similar enhancement for this quantity also in model II. For example, $\epsilon'_{\gamma\gamma(-)}/\eta$ is two orders of magnitude greater than the SM result for $\xi = 8$ and $m_H \simeq m_t$. We also see from these graphs that as the ratio m_H/m_t goes to infinity the direct CP-violating parameter $\epsilon'_{\gamma\gamma(-)}$ tends to SM predictions in both models.

For the B-meson decay $\epsilon'_{\gamma\gamma(-)}$ is defined analogously to the K-meson case. Since the parameter λ_u is small in B decay one finds

$$\epsilon'_{\gamma\gamma(-)} = \frac{\mathrm{Im}\lambda_t}{\mathrm{Re}\lambda_t} = \frac{A\lambda^4\eta}{-A\lambda^2} \simeq -\lambda^2\eta = -4.8\times10^{-2}\,\eta \,. \tag{25}$$

Note that this expression is the same as the one in SM, and with $0.2 < \eta < 0.5$, it is quite measurable at the future B-meson factories.

In the end we would like to mention some related decays, namely, $B_s \to \mu^+\mu^-$ [19] and $B_s \to \tau^+\tau^-$ [20], which are of the same order of α as $B_s \to \gamma\gamma$ decay. In order to compare our results with those given by Refs. [19] and [20] we present in Fig. 13 the m_H dependence of the branching ratio for $B_s \to \gamma\gamma$ decay in the case that the amplitude gets a contribution only from the charged Higgs bosons. We see that at $\xi = 3$ and $m_H = 200$ GeV we have

$$B(B_s \to \gamma\gamma) \simeq 10^{-6} \,. \tag{26}$$

At the same values of parameters,

$$B(B_s \to \mu^+\mu^-) \simeq 4\times10^{-9} \,. \tag{27}$$

It is well known that between $B_s \to \mu^+\mu^-$ and $B_s \to \tau^+\tau^-$ decays the following relation holds true:

$$B(B_s \to \tau^+\tau^-) \simeq \left(\frac{m_\tau}{m_\mu}\right)^2 B(B_s \to \mu^+\mu^-) \simeq 3\times10^2 B(B_s \to \mu^+\mu^-) \simeq 10^{-6} \,.$$

So we see that branching ratios of the $B_s \to \gamma\gamma$ and $B_s \to \tau^+\tau^-$ decays have the same order of magnitude and they are larger than the branching ratio of $B_s \to \mu^+\mu^-$ by two orders of magnitude in the considered region.

In conclusion, we note that the extended Higgs sector is one of the possible sources of the enhancement of the flavor-changing transitions. The other source may be the fourth generation. But it does not lead to any strong enhancement for the considered decay because it is determined by the magnetic-dipole-type operator F_2, which decreases for $\alpha \gg 1$. This means that great enhancement of the B for $B_s \to \gamma\gamma$ decay indicates the existence of the extended Higgs sector. Therefore, the radiative rare decays of the B mesons may be efficient tools for establishing the extended Higgs sector.

[1] J. F. Gunion *et al.*, *The Higgs Hunter's Guide* (Addison-Wesley, Reading, MA, 1990).

[2] R. D. Peccei and H. R. Quinn, Phys. Rev. D **16**, 1791 (1977); S. Weinberg, Phys. Rev. Lett. **40**, 223 (1978); F. Wilczek, *ibid.* **40**, 279 (1978); J. Kim, *ibid.* **43**, 103 (1979).

[3] C. Froggat, R. G. Moorhouse, and I. G. Knowles, Nucl. Phys. **B386**, 63 (1992).

[4] G. L. Lin, J. Liu, and Y. P. Yao, Phys. Rev. D **42**, 2314 (1990).

[5] S. Herrlich and J. Kalinowski, Nucl. Phys. **B381**, 501 (1992).

[6] S. L. Glashow and S. Weinberg, Phys. Rev. D **15**, 1958 (1977).

[7] H. Haber, G. Kane, and T. Sterling, Nucl. Phys. **B161**, 493 (1979).

[8] J. Gunion and H. Haber, Nucl. Phys. **B272**, 1 (1986).

[9] S. Weinberg, Phys. Rev. D **42**, 860 (1990).

[10] E. Ma and A. Pramudita, Phys. Rev. D **24**, 2476 (1981).
[11] T. M. Aliev and V. L. Eletsky, Yad. Fiz. **38**, 1537 (1985) [Sov. J. Nucl. Phys. **38**, 936 (1983)].
[12] M. Neubert, Phys. Rev. D **45**, 2451 (1992).
[13] C. Alton *et al.*, Nucl. Phys. **B349**, 598 (1991); C. Alexandrou *et al.*, Phys. Lett. B **256**, 60 (1991); E. G. Bernard *et al.*, Phys. Rev. D **38**, 3540 (1988).
[14] Particle Data Group, K. Hikasa *et al.*, Phys. Rev. D **45**, S1 (1992).
[15] B. Grzadkowski, J. Gunion, and P. Krawckyk, Phys. Lett. B **268**, 106 (1991); J. Gunion and B. Grzadkowski, *ibid.* **243**, 301 (1990); V. Barger, J. Hewett, and R. J. N. Phillips, Phys. Rev. D **41**, 3421 (1990).
[16] D. Cocolicchio and J. Cudell, Phys. Lett. B **245**, 591 (1990); A. Buras, P. Krawczyk, M. Lautenbacker, and C. Salazar, Nucl. Phys. **B337**, 284 (1990).
[17] L. Wolfenstein, Phys. Rev. Lett. **51**, 1945 (1983).
[18] A. Ali, J. Phys. G **18**, 1605 (1992); A. J. Buras and M. K. Harlander, Report No. MPI-PAE/PTh 1/92 TUM-T31-25/92 (unpublished).
[19] J. H. Hewett, S. Nandi, and T. G. Rizzo, Phys. Rev. D **39**, 250 (1989).
[20] G. Eliam and A. Soni, Phys. Lett. B **215**, 171 (1988).